Articles

Phosphorylation Changes the Spatial Relationship between Glu124−Arg143 and Cys18 and Cys165 of the Regulatory Light Chain in Smooth Muscle Myosin[†,‡]

Guanming Wu,[§] Anna Wong,[§] Fang Qian,[§] and Renne Chen Lu*[,§,||]

Muscle Research Group, Boston Biomedical Research Institute, Boston, Massachusetts 02114, and Department of Neuropathology, Harvard Medical School, Boston, Massachusetts 02115

Received January 8, 1998; Revised Manuscript Received March 11, 1998

ABSTRACT: Regulatory light chain (RLC) mutants, RLC-C18 and RLC-C165, containing a single cysteine at positions 18 and 165 near the N and C terminus, respectively, were each labeled with benzophenone 4-iodoacetamide and exchanged into myosin in their phosphorylated or unphosphorylated forms and then photolyzed. SDS−PAGE showed that, for RLC-C18, the intrachain photo-cross-linking in myosin was inhibited by phosphorylation. For myosin containing RLC-C165, the yield of one intrachain cross-linked band decreased significantly whereas the other was unaffected by phosphorylation. Peptide mapping in conjunction with mass spectrometry showed that Cys165 was cross-linked to site(s) within Ala17−Lys34 independent of the phosphorylation of Ser19. This clearly demonstrates that the proximity between the N- and C-terminal regions of RLC is not affected by phosphorylation. In addition, Cys165 could also be cross-linked to the region of Phe133−Arg143; however, this type of cross-linking was inhibited in the phosphorylated state. For RLC-C18, the cross-linking took place with the region of Glu124−Arg132 or Phe133−Arg143, also only in the unphosphorylated state. Thus, phosphorylation changes the spatial relationship between the region of Glu124−Arg143 and Cys18 and Cys165. In scallop myosin, the region corresponding to Glu124−Arg143 is located at the interfaces between RLC and the essential light chain as well as the heavy chain [Xie, X., et al. (1994) *Nature 368*, 306−312]. In light of that work, our results suggest that the region of Glu124−Arg143 is involved in the phosphorylation-dependent signaling and the change in its spatial relationship with respect to the N and C termini of RLC may underlie the activation of the smooth muscle myosin.

Myosin from chicken gizzard smooth muscle, similar to myosin from skeletal muscle, is made of two heavy chains with a chain weight of 200 kDa each and two pairs of light chains, designated as regulatory light chains (RLC)[1] and essential light chains (ELC), with chain weights of 20 and 17 kDa, respectively. Each N-terminal portion of the heavy chains, about 95 kDa, is folded into a pear-shaped head; together with a pair of the light chains, they are called subfragment-1 (S1), and the rest of the two heavy chains are joined in a coiled-coil α-helical rod. The heavy chains of S1 can be cleaved with proteolytic enzymes into three fragments with apparent masses of 25, 50, and 20 kDa on SDS−PAGE (*3*, *4*). It has been well established that the phosphorylation of RLC is essential for initiation of the force development of smooth muscle (*5*), and Ser19 of RLC has been identified as the phosphorylation site responsible for the regulation (*6*). However, the mechanism of phosphorylation regulation remains unclear.

The atomic structure of S1 from chicken skeletal muscle was reported by Rayment et al. (*7*). One key feature of the S1 structure is a long helix (∼85 Å) in the 20 kDa region, which extends from the globular part of the head to the head−rod joint. The two light chains wrap around the C-terminal portion of the long helical segment, forming the so-called "regulatory domain". The rest of the 20 kDa region together with the 50 and 25 kDa regions forms the globular portion of the head, which contains both the actin and nucleotide binding sites and is therefore referred to as the catalytic or motor domain. In both structures of chicken myosin S1 or the regulatory domain of the scallop myosin (*8*), the RLC is folded into two domains, each domain making tight contact with the helical heavy chain. Whereas the general features of the smooth muscle RLC are likely to

[†] Supported by National Institutes of Health Grants AR28401, AR41637, and RR11301 and National Science Foundation Grant 9604781.

[‡] The preliminary work has been presented at the Annual Meetings of the Biophysical Society (*1*, *2*).

* To whom correspondence should be addressed: Boston Biomedical Research Institute, 20 Staniford St., Boston, MA 02114. Telephone: (617) 912-0379. Fax: (617) 912-0308. E-mail: Lu@bbri.harvard.edu.

[§] Boston Biomedical Research Institute.

[||] Harvard Medical School.

[1] Abbreviations: RLC, regulatory light chains; ELC, essential light chains; S1, subfragment-1; PCR, polymerase chain reaction; IPTG, isopropyl 1-thio-β-D-galactopyranoside; BPIA, benzophenone 4-iodoacetamide; MLCK, myosin light chain kinase; MALDI-TOF MS, matrix-assisted laser desorption/ionization time-of-flight mass spectrometry; PSD, post-source decay; PVDF, polyvinylidene difluoride.

S0006-2960(98)00054-3 CCC: $15.00
Published on Web 05/07/1998

be similar to those of skeletal and scallop RLC, there is no information in the published structures relevant to the N-terminal 25-amino acid segment of the smooth muscle RLC which contains the phosphorylation site (Ser19). This makes it difficult to predict the location of the phosphorylation site and the phosphorylation-induced structural changes. Consequently, how the phosphate group at the neck region of myosin can affect the ATPase site which is at the distal end of the myosin head remains unknown. To delineate the signaling pathway between the phosphorylation site and ATPase site, we began our studies with single cysteine RLC mutants and photo-cross-linking techniques followed by SDS−PAGE and peptide mapping in conjunction with mass spectrometry to identify phosphorylation-dependent structural changes. Our results indicate that, while the proximity between the phosphorylation region and the Cys165 of RLC is not affected by phosphorylation, the spatial relationship of the segment of Glu124−Arg143 with respect to Cys165 and Cys18 is altered due to the phosphorylation of Ser19. The significance and implications of our findings are discussed with respect to the crystal structure of the regulatory domain of the scallop myosin (*8*).

MATERIALS AND METHODS

Construction of RLC Cysteine Mutants. The chicken gizzard cDNA library was kindly supplied by S. Hughes (National Cancer Institute, Frederick, MD). The constructs of single cysteine mutants were obtained by replacing the endogenous Cys108 with Ala and then replacing Gly165 or Thr18 with Cys using the PCR overlapping extension method (*9*). All mutants were full-length sequenced using the Sequenase Kit (U.S. Biochemical Corp.) to verify the mutagenesis. Wild type and mutant RLC cDNAs were cloned into expression vector pAED4 (*10*) and expressed in *Escherichia coli* BL21 (DE3) cells using IPTG (isopropyl 1-thio-β-D-galactopyranoside) as an inducer.

Purification of Expressed Proteins. Recombinant light chains were extracted using the procedure of Wolff-Long et al. (*11*). The pellet was solubilized in a buffer containing 30 mM Tris-HCl (pH 7.5), 10 mM DTT, and 4 M urea and the mixture stirred gently for 30 min at room temperature. Insoluble material was removed by centrifugation at 100000*g* for 30 min. The supernatant was applied to a DE-52 column (2.5 × 20 cm) equilibrated in 7 M urea containing 50 mM NaCl, 1 mM DTT, and 30 mM Tris-HCl (pH 7.5). Proteins were eluted with a linear gradient of NaCl from 0.05 to 0.3 M (total volume = 500 mL). Fractions containing RLC were determined by SDS−PAGE, pooled, and dialyzed against 5 mM ammonium bicarbonate and 1 mM DTT extensively at 4 °C. After centrifugation at 100000*g* for 20 min, the light chains were lyophilized and stored at −20 °C.

Modification of Light Chains with BPIA. Lyophilized recombinant RLC was dissolved in 30 mM KCl, 30 mM Tris-HCl (pH 7.5), and 1 mM EDTA to a concentration of 2.0 mg/mL and clarified at 100000*g* for 30 min. RLCs were modified with a 5-fold molar excess of BPIA (purchased from Molecular Probes, Junction City, OR). The reaction was allowed to proceed for 45 min at room temperature and then stopped by the addition of a 10-fold molar excess of DTT to BPIA. Excess reagents were removed by extensive dialysis against 0.3 M NaCl, 30 mM Tris-HCl (pH 7.5), and 0.5 mM DTT followed by centrifugation at 100000*g* for 20 min. Unmodified RLC was used to generate a standard curve in the Bradford protein assay (kits purchased from Bio-Rad) to determine the concentration of modified light chains.

The extent of labeling was determined using the absorbance at 300 nm and the molar extinction coefficient of 23 × 10^3 for the BP moiety.

Phosphorylation. Labeled RLC was incubated with myosin light chain kinase (MLCK) and calmodulin at 25 °C for 30 min in a buffer containing 1 mM ATP, 1 mM $MgCl_2$, 0.1 mM $CaCl_2$, 0.3 M NaCl, and 30 mM Tris-HCl (pH 7.5) (*12*). All samples were dialyzed against 50 mM NaCl, 30 mM Tris-HCl (pH 7.5), and 0.5 mM DTT. The extent of phosphorylation was monitored by urea gel electrophoresis (*13*). Myosin prepared from chicken gizzard and unlabeled RLCs were also phosphorylated as controls. MLCK was copurified with the native caldesmon from chicken gizzard first and then purified on a phosphocellulose P-11 column (Whatman) after separation from the native caldesmon on a TSK DEAE-650S column (Supelco) as described by Graceffa (*14*). The completeness of the phosphorylation was routinely monitored by urea gel electrophoresis (see below).

Protein Preparations. Smooth muscle myosin was prepared from frozen chicken gizzards obtained from Pell-Freeze as described by Ikebe et al. (*15*). Actin was prepared from rabbit skeletal muscle according to Spudich and Watt (*16*), and tropomyosin was prepared from chicken gizzard as described by Graceffa (*17*). Protein concentrations were determined spectrophotometrically using an E_{290} of 0.63 for actin (1 mg/mL) and an E_{277} of 0.19 for gizzard tropomyosin (1 mg/mL). E_{277} = 0.337 for RLC (1 mg/mL), and E_{277} = 0.45 for myosin (1 mg/mL).

Exchange of RLC into Myosin. Myosin and the modified RLC with a molar ratio of 1:15 in a buffer containing 30 mM Tris-HCl (pH 7.5), 0.5 M NaCl, 10 mM ATP, 10 mM EDTA, and 10 mM DTT were incubated at 40 °C for 30 min as described by Morita et al. (*18*). The samples were then dialyzed against 30 mM Tris-HCl (pH 7.5), 15 mM $MgCl_2$, and 1 mM DTT to precipitate the myosin. The precipitated myosins were collected by centrifugation, washed twice with dialysis buffer, resuspended in 0.3 M NaCl, 30 mM Tris-HCl (pH 7.5), and 1 mM DTT, then dialyzed overnight at 4 °C, and clarified by centrifugation. Unphosphorylated and phosphorylated unlabeled RLCs were also exchanged into myosin as controls. The completeness of the exchange was determined by analysis on glycerol−acrylamide gels (see below).

Gel Electrophoresis. SDS−PAGE was carried out on Bio-Rad Mini-PROTEAN II and Hoefer SE600 16 cm slab units containing a 4% stacking and 12% running gel; gel electrophoresis was performed in Tris-Bicine buffer (pH 8.4), and the other conditions were similar to those of the procedure of Laemmli (*19*). For the urea gel system, the running gel contained 4 M urea and 8.5% acrylamide with a 5.4% stacking gel. For the glycerol gel system, the running gels contained 40% (v/v) glycerol and 10% total acrylamide (with 5% of the total as bisacrylamide) with a 4.5% stacking gel (*13*). Both the urea and glycerol gels were run in a buffer containing 40 mM Tris-glycine (pH 8.6). The samples for glycerol−acrylamide gels were precipitated with trichloro-

acetic acid first and resolubilized in an 8 M urea sample buffer as described by Trybus and Lowey (*20*).

Electroblotting. After electrophoresis on 12% running gels, the proteins were blotted onto Immobilon PVDF (Millipore) using a Bio-Rad Trans-Blot Cell with 10 mM CAPS (pH 11.0) and 10% methanol as the transfer buffer. A strip was cut out and stained with 0.1% Coomassie Blue R in 50% methanol which was used as a guide for excising the protein bands.

Tryptic Digestion. For blotted samples, unstained protein bands were digested with trypsin (0.02 mg/mL, TPCK−trypsin from Worthington) in 10% acetonitrile, 100 mM Tris-HCl (pH 8.0), and 1% octyl glucopyranoside (Sigma) at 37 °C for 20 h. The tryptic peptides were extracted using the procedure of Gharahdaghi et al. (*21*). Chymotryptic digestion was perfomed under the same conditions, except 0.04 mg/mL chymotrypsin (α-chymotrypsin from Worthington) was used.

Microbore HPLC. Peptide mixtures of myosin or light chains were fractionated on a Hewlett-Packard microbore model 1090 HPLC apparatus using a Vydac C18 column (2.1 × 250 mm). The peptides of myosin were eluted with a 90 min gradient of 0 to 60% acetonitrile in 0.1% TFA with a flow rate of 100 μL/min; the reaction was monitored at wavelengths of 214, 254, 280, and 300 nm, and 2 min fractions were collected. The peptides of the light chains were fractionated similarly, except they were eluted with a 60 min gradient.

Mass Spectrometry. Mass analyses of the fractionated peptides were performed on a matrix-assisted laser desorption/ionization time-of-flight (MALDI-TOF) mass spectrometer system from Perseptive Biosystems (model Voyager-RP). Both sinapinic acid and α-cyano-4-hydroxycinnamic acid were purchased from Aldrich and were used for protein and peptides, respectively. Nonionic detergent *n*-octyl β-D-glucopyranoside was included in the matrix solution as described by Cohen and Chait (*22*). The mass spectra were obtained in the linear mode using positive ion detection with a mass accuracy of 0.1%. Human angiotensin II with a mass of 1047.18 Da and bovine insulin with a mass of 5734.50 Da were purchased from Sigma and were used as calibration standards.

Structure information about a molecule may be obtained by analyzing the fragment ions that dissociate from the original ion (precursor) in the flight tube in the reflective state of MALDI-TOF mass spectrometry, known as the post-source decay (PSD) analysis. The timed ion selector feature of the Voyager-RP instrument allows one to selectively analyze the mass species of interest, without interference from other mass species in the sample. The assignments of the cross-linked peptides based on the spectra in the linear mode were verified by sequence information obtained using the PSD mode. The PSD analyses were performed using a series of PSD mirror ratio values and parameters as described in the user's guide provided by the manufacturer.

Other Procedures. To ascertain the mutants and mutants labeled with the BP moiety that retained the function of RLC, the phosphorylation-activated actomyosin ATPase activity was routinely monitored for each mutant. Actin-activated Mg^{2+}-ATPase activities were determined using the following conditions: 14 mM Tris-HCl (pH 7.5), 90 mM NaCl, 2 mM $MgCl_2$, 0.1 mM $CaCl_2$, 6 mM DTT, 0.24 mg of myosin, 93 μg of actin, 45 μg of tropomyosin, and 2 mM ATP (*23*). Photolysis was carried out for 30 min at 4 °C in a Rayonet RPR-100 photochemical reactor equipped with 16 "3500" lamps (Southern New England Ultraviolet, Hamden, CT).

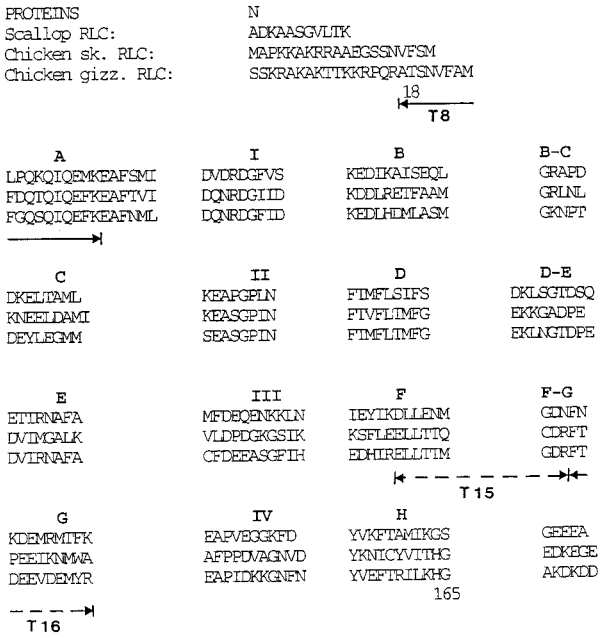

FIGURE 1: Alignment of amino acid sequences of RLC from chicken gizzard (*32*), chicken skeletal (*33*), and scallop (*34*) myosins based on the helix−loop−helix motif. I−IV are four divalent cation binding loops, and A and B, C and D, E and F, and G and H represent the four pairs of flanking helices, respectively. Numbers 18 and 165 mark the residues that were replaced with cysteines. The solid line designated with T8 shows the region that was cross-linked to Cys165 in both the phosphorylated and unphosphorylated state. The broken line designated with T15 and T16 indicates these two regions could be cross-linked to Cys18 and Cys165 only in the unphosphorylated state.

RESULTS

Generation of the Single Cysteine Mutants RLC-C165 and RLC-C18. The primary structure of the regulatory light chain is highly homologous to other calcium binding proteins such as calmodulin and troponin C. The crystal structures of chicken skeletal myosin subfragment-1 (*7*) and the scallop myosin regulatory domain (*8*) confirmed that RLCs also share structural homology with calmodulin and troponin C, consisting of two domains each containing two helix−loop−helix (EF-hand) motifs which wrap around the helical heavy chain. Figure 1 shows the primary structures of RLCs from scallop, chicken skeletal, and chicken gizzard myosin aligned according to the EF-hand motif. Each of the putative divalent ion binding loops, designated I−IV, is flanked with two helical regions, referred to as A and B, C and D, E and F, and G and H, respectively.

Selection of position 165 as a site for the mutation was based on the following rationale. First, the crystal structures of RLCs from scallop and skeletal myosin indicated that this residue is not directly involved in calcium or heavy chain binding, and thus, replacing this residue with a cysteine is unlikely to impair the functions of RLC. Second, previous studies implied that the C-terminal domain of RLC is essential for smooth muscle regulation, and thus, position 165 would be a strategically important site for monitoring

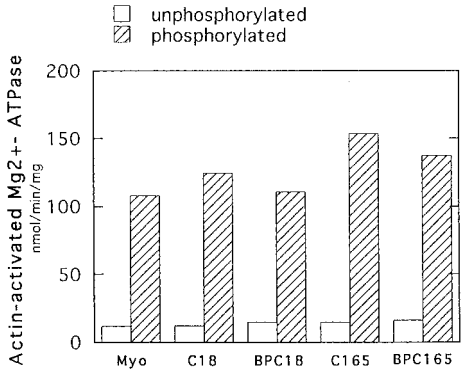

FIGURE 2: Actin-activated Mg^{2+}-ATPase activity of myosin prepared from chicken gizzard myosin and myosin containing RLC-C18, BP−RLC-C18, RLC-C165, or BP−RLC-C165. The activities of unphosphorylated myosins are shown in open bars, and those of phosphorylated myosins are shown in cross-hatched bars. All values were derived from averaging four measurements except that of gizzard myosin which was the average of eight measurements.

structural changes induced by phosphorylation. Third, although residue 165 is the seventh residue from the C terminus, it is at the edge of the H helix, and therefore, the probe would be at a position with relatively stable secondary structure.

Thr18 was chosen for substitution with Cys because it is next to the phosphorylation site, Ser19. Probes placed at Cys18 will not only sense the conformation change near the phosphorylation site but also provide information on the structure of the N-terminal region which is lacking from the crystal structures of chicken skeletal RLC (*7*) and scallop RLC (*8*).

Mutants RLC-C165 and RLC-C18 retained the properties of wild type RLC. Actin-activated myosin Mg-ATPase activities showed that myosin containing either RLC-C165 or RLC-C18 was fully activated by phosphorylation, and modification with BPIA did not affect the phosphorylation-dependent regulation (Figure 2).

Photo-Cross-Linking of Myosin Containing RLC-C165. In the free state, almost all of the RLC-C165 became intrachain cross-linked and appeared on SDS−PAGE as two bands with mobilities higher than that of un-cross-linked RLC (Figure 3, lane b), indicating that at least two different regions can be cross-linked to Cys165. Phosphorylation did not affect either the yield or the pattern of the intrachain cross-linking in the free state (Figure 3, lane c). In the bound state, a significant amount of the RLC appeared on SDS−PAGE with a mobility identical to that of un-cross-linked RLC, indicating that intrachain cross-linking of RLC decreased when RLC was associated with the heavy chain (Figure 3, lane d). Upon phosphorylation, the yield of the intrachain cross-linked RLC with lower mobility, XL1, decreased significantly whereas that of the other, XL2, was apparently not affected (Figure 3, lane e). No cross-linked products corresponding to RLC cross-linked to the heavy chains were observed whether or not RLC was phosphorylated. Since the extent of labeling and the completion of exchange were the same for myosin containing the phosphorylated and unphosphorylated RLC-C165, the decrease in the yield of one of the cross-linked products clearly revealed the phosphorylation-induced structural changes in RLC. The fact that only one (XL1) of the two cross-linked bands was affected by phosphorylation further ruled out the possibilities that the

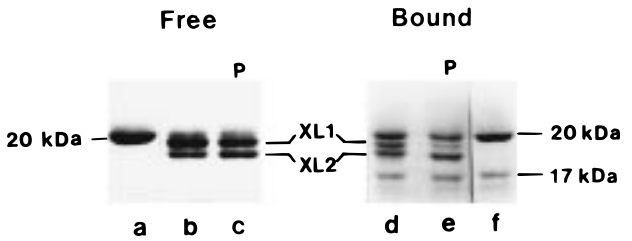

FIGURE 3: SDS−PAGE analysis of RLC-C165 labeled with BPIA and photolyzed in the free and bound states. Experiments were carried out in 0.15 M NaCl, 30 mM Tris-HCl (pH 7.5), 1 mM DTT, and 2 mM $MgCl_2$: lane a, BP−RLC-C165 before photolysis; lane b, unphosphorylated BP−RLC-C165 photolyzed for 30 min; lane c, phosphorylated BP−RLC-C165 photolyzed for 30 min; lane d, myosin containing unphosphorylated BP−RLC-C165 photolyzed for 30 min; lane e, myosin containing phosphorylated BP−RLC-C165 photolyzed for 30 min; and lane f, control, chicken gizzard myosin. The labels 20 and 17 kDa refer to RLC and ELC, respectively, and XL1 and XL2 refer to the slower and faster moving band on SDS−PAGE of the intrachain cross-linked RLC, respectively.

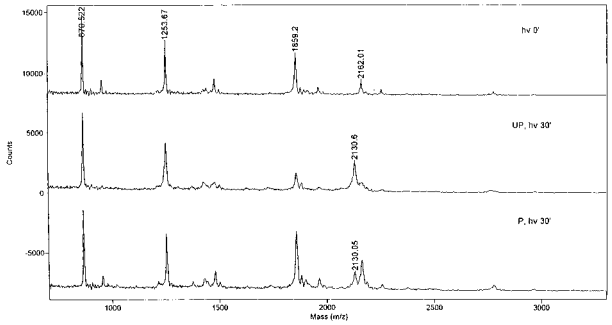

FIGURE 4: Mass analysis of the tryptic digests of myosin containing RLC-C165 on a MALDI-TOF mass spectrometer. Spectra were obtained from the HPLC fraction that eluted at 47−48 min of myosin containing phosphorylated RLC-C165 before photolysis (top spectrum) and after photolysis (bottom spectrum). The spectrum of the corresponding fraction of myosin containing the unphosphorylated RLC-C165 after photolysis is shown in the middle. The complete spectra covered the mass range from 0 to 20 000 Da, and only the relevant sections are shown.

decrease in the yield of XL1 type cross-linked products resulted from incomplete labeling or less efficient exchange of the phosphorylated RLC-C165. The absence of a phosphorylation effect on the cross-linking in the free state indicates that phosphorylation-induced structural changes occur in RLC bound to the heavy chains.

Identification of the Regions That Are Cross-Linked to Cys165. Photolyzed and unphotolyzed myosin samples containing RLC-C165 were cleaved with trypsin and then subjected to microbore HPLC using a Vydac C18 column; the elution profiles were similar in both cases (data not shown). An aliquot from each fraction was analyzed on a Voyager-RP mass spectrometer. The distributions of various kinds of mass species in each fraction of the photolyzed sample were similar to that of the corresponding fraction from the unphotolyzed sample for the most part. Efforts were made to identify the mass species that were present only in the photolyzed samples. The spectrum of the fraction that eluted at 47−48 min of the photolyzed sample showed an extra peak at 2130.60 Da (Figure 4, middle spectrum), in comparison with the spectrum of the unphotolyzed sample (Figure 4, top spectrum). Since the cross-linker was attached to T21 (His164−Lys167), any peptide that was cross-linked

Table 1: Masses of the Tryptic Peptides of the Regulatory Light Chain and Cross-Linked Peptides in RLC-C165 and RLC-C18

peptide	residue	mass + 1[a] (Da)	+BPT21[b] in RLC-C165 (Da)	+BPT8[c] in RLC-C18 (Da)
T1	1−3	321.34	1015.99	2651.76
T2	4	175.20	869.85	2505.62
T3	5 and 6	218.27	912.85	2548.69
T4	7 and 8	218.27	912.85	2548.69
T5	9−11	349.40	1044.05	2679.82
T6	12	147.19	841.84	2477.61
T7	13−16	556.64	1251.29	2887.06
T8	17−34	2092.32[c]	2786.97	4661.84
T9	35−44	1238.35	1933.00	3568.77
T10	45−50	694.75	1389.40	3025.17
T11	51−62	1347.53	2042.18	3677.95
T12	63−92	3399.87	4094.62	5730.29
T13	93−103	1229.32	1923.97	3559.74
T14	104−123	2277.40	2972.05	4607.82
T15	124−132	1036.18	1730.83	3366.60
T16	133−143	1434.51	2129.16	3764.93
T17	144−149	672.75	1367.40	3003.17
T18	150	147.19	841.84	2477.61
T19	151−160	1247.34	1941.99	3577.76
T20	161−163	373.51	1068.16	2703.93
T21	164−167	412.46[b]	1390.30	2742.88
T22	168 and 169	262.28	956.93	2592.70
T23	170 and 171	249.19	943.84	2579.61

[a] This column shows the calculated masses of tryptic peptides of the wild type regulatory light chain from chicken gizzard myosin except Cys108 in T14 has been replaced with Ala. [b] In RLC-C165, Gly165 was replaced with Cys and the BP moiety is attached to Cys165 which is located in T21. The mass of T21 in RLC-C165 is 457.55 Da. The mass of any peptide that is cross-linked to Cys165 will increase by 694.65 Da, the sum of the mass of T21, and 237.10 Da, the mass of BPIA minus the mass of HI. [c] In RLC-C18, Thr18 was replaced with Cys and Cys18 is located in T8. Thus, the mass of any of the peptides that is cross-linked to Cys18 will increase by 2330.42 Da, the sum of the mass of T8 in RLC-C18, 2093.32 Da, plus 237.10 Da, the mass of BPIA minus the mass of HI.

to Cys165 would increase by the mass of T21 and the moiety of benzophenone acetamide, 694.65 Da. Thus, the fragment with a mass of 2130.60 Da most likely corresponded to T21 cross-linked to T16, which has a calculated mass of 2129.16 Da (Table 1). The mass peak at 2130 Da also appeared in phosphorylated myosin, although the peak height was consistently smaller (Figure 4, bottom spectrum). However, no conclusion should be drawn concerning the yields of the cross-linked products on the basis of these analyses since the peak heights are not necessarily proportional to their concentration in the sample.

Post-source decay (PSD) analysis of a targeted mass peak (precursor) allows one to detect the mass fragments generated during mass spectrometry (MS) and thus confirm the sequence of the precursor. The MS fragmentation does not always occur at the typical peptide bond as in the case of Edman degradation. However, the most commonly detected mass fragments result from cleavages of the peptide bonds with the retention of the N terminus (b ions) or the C terminus (y ions). When the PSD spectrum of precursor 2130 was examined, ions with masses matched with b3−b5, b7, y1, y2, and T16 (Table 2) were found. In addition, ions with masses corresponding to internal dipeptides of T16 such as DE (244.59 Da) and EE (259.2 Da) as well as characteristic ions of His (109 Da) and Lys (128 Da) were also found. Most importantly, the ions, designated y3*−y8* (except y6*), with masses matched with y ions cross-linked to T21 were identified (Table 2). Thus, the results unambiguously confirmed the initial assignment that mass species 2130 Da was made of T16 cross-linked to T21. Further, the presence of b7 and y2 ions strongly suggested that the first seven amino acids from the N terminus and the last two amino acids from the C terminus of T16 were not involved in cross-linking, which implied that Glu140 and Met141 were involved in cross-linking. The fact that all y* ions contain Met141 led us to conclude that Met141 was the primary cross-linking site in this region, although the involvement of Glu140 could not be ruled out.

The spectrum of the fraction that eluted at 58−59 min also showed one additional peak with a mass of 2786.85 Da in the photolyzed myosin (Figure 5, middle spectrum), in comparison with the unphotolyzed myosin (Figure 5, top spectrum), which matched well with the mass of 2786.97 Da, corresponding to T21 cross-linked to T8 (Table 1). In the phosphorylated sample, a peak appeared at 2866 Da instead of at 2786 Da (Figure 5, bottom spectrum); the increase of 80 Da is equivalent to that of a phosphate moiety, indicating that T21 could be cross-linked to phosphorylated T8 as well. Thus, the results showed that cross-linking

Table 2: Mass Ions of T16 and T16 Cross-Linked to T21[a]

n	Fragments	b (cal)	observed	Fragments	y (cal)	observed	y* (cal)	observed
1	F	148.18		R	175.21	174.74	869.86	
2	FT	249.29		YR	338.38	337.68	1033.03	
3	FTD	364.38	363.91	MYR	469.57		1164.22	1165.27
4	FTDE	493.49	492.70	EMYR	598.69		1293.34	1292.49
5	FTDEE	622.61	622.14	DEMYR	713.78		1408.43	1408.13
6	FTDEEV	721.74		VDEMYR	812.91		1507.56	
7	FTDEEVD	836.83	836.49	EVDEMYR	942.02		1636.67	1635.43
8	FTDEEVDE	965.94		EEVDEMYR	1071.14		1765.79	1765.29
9	FTDEEVDEM	1097.14		DEEVDEMYR	1186.23		1880.88	
10	FTDEEVDEMY	1260.31		TDEEVDEMYR	1287.33		1981.98	
T16	FTDEEVDEMYR	1434.51	1434.04	FTDEEVDEMYR	1434.51	1434.04	precursor	2130.24

[a] Values of y*n** ions were derived from the mass of the y*n* ion plus the mass of BP-T21 (694.65 Da).

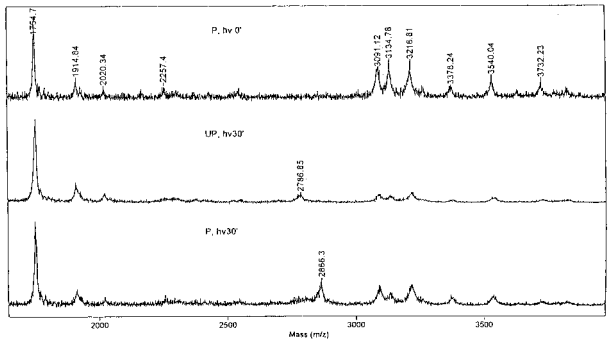

FIGURE 5: Mass analysis of the tryptic digests of myosin containing RLC-C165 on a MALDI-TOF mass spectrometer. Spectra were obtained from the HPLC fraction that eluted at 58−59 min of the tryptic digests of myosin containing phosphorylated RLC-C165 before photolysis (top spectrum) and after photolysis (bottom spectrum). The spectrum of the corresponding fraction of myosin containing the unphosphorylated RLC-C165 after photolysis is shown in the middle. The complete spectra covered the mass range from 0 to 20 000 Da, and only the relevant sections are shown.

between Cys165 and the region of Ala17−Lys34 was not affected by phosphorylation.

In the free state, cross-linking took place between Cys165 and T9, T10, T11, T12, and T15 as well as T8 and T16 (data not shown), and similar results were obtained for phosphorylated RLC-C165. These results indicate that the RLC molecule is much more flexible in the absence of the heavy chains. The absence of a phosphorylation effect on the cross-linking products analyzed by mass spectrometry is consistent with the cross-linking pattern observed on SDS−PAGE (Figure 3).

Identification of the Cross-Linked Products Inhibited by Phosphorylation. The fact that cross-linking between Cys165 and the region of Ala17−Lys34 was not affected by phosphorylation suggests that this type of the cross-linked product would correspond to XL2 on SDS−PAGE, which was not affected by phosphorylation (Figure 3). To confirm this and to determine whether RLC containing cross-links between Cys165 and the region of Phe133−Arg143 corresponded to the cross-linked products with lower mobility on SDS−PAGE, XL1, unstained bands correponding to XL1 and XL2 (Figure 3, lane d) were cut out according to the guide strip and cleaved with trypsin and the tryptic peptides were chromatographed on HPLC followed by analyses on a Voyager-RP spectrometer. The mass peak at 2128.97 Da was found in the 38−40 min fraction of XL1, but not in XL2 (Figure 6, left panel). Thus, it is clear that cross-linking between Cys165 and T16 resulted in RLC with a mobility like that of XL1 which was inhibited upon phosphorylation as shown by SDS−PAGE (Figure 3). The phosphorylation-induced inhibition of the cross-linking between Cys165 and T16 is unique to RLC bound to the heavy chain since in the free state phosphorylation does not affect the cross-linking pattern (Figure 3).

As expected, Cys165 cross-linked to T8 with a mass of 2786.79 Da was found in the fraction that eluted between 48 and 50 min of the tryptic digest of XL2, but not in the corresponding fraction of XL1 (Figure 6, right panel) of unphosphorylated RLCs. The corresponding fraction of phosphorylated XL2 (Figure 3, lane e) showed a mass peak at 2865.91 Da which corresponded to T21 cross-linked to phosphorylated T8 (Figure 6, right panel, bottom spectrum). These results indicated that T21 was cross-linked to T8, whether or not it was phosphorylated, consistent with the

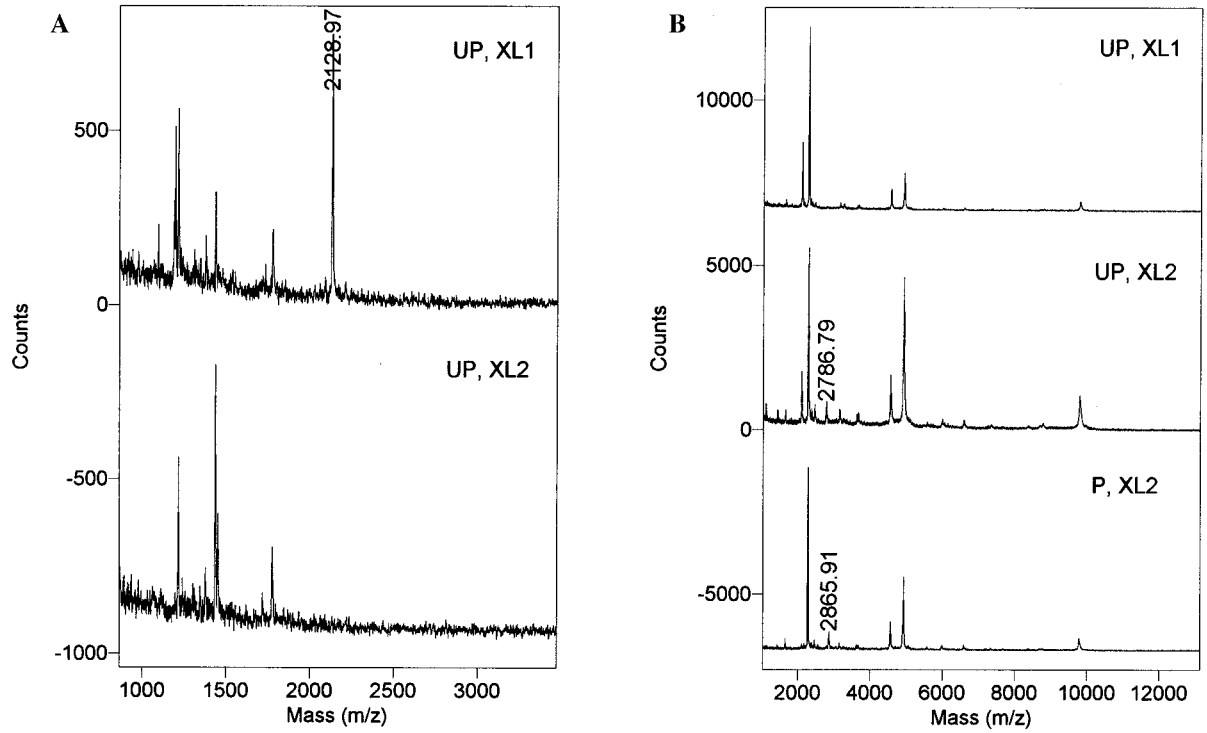

FIGURE 6: (A) Section of the spectra of MALDI-TOF analysis of the fraction that eluted at 38−40 min of the tryptic digest of the cross-linked RLC-C165 of myosin. The top and bottom traces were derived from XL1 and XL2, respectively, of RLC-C165 (Figure 3, lane d). (B) Section of the spectra of MALDI-TOF analysis of the fraction that eluted at 48−50 min of the tryptic digest of the photo-cross-linked RLC-C165 of myosin. The top and middle traces were derived from XL1 and XL2, respectively (Figure 3, lane d); the bottom trace was derived from XL2 of phosphorylated RLC-C165 (Figure 3, lane e).

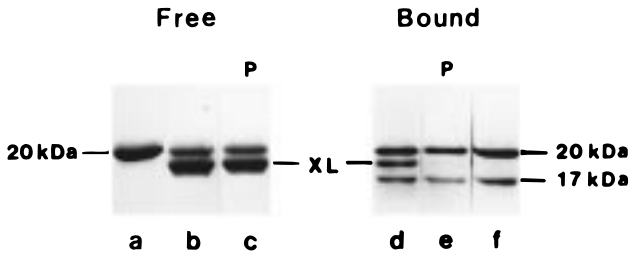

FIGURE 7: SDS-PAGE analysis of gizzard myosin (lane f) and RLC-C18 labeled with BPIA before photolysis (lane a) and after it was photolyzed for 30 min in the free (lanes b and c) and bound states (lanes d and e). Lanes b and d were unphosphorylated samples, and lanes c and e were phosphorylated samples. Experimental conditions were the same as in Figure 3. XL refers to cross-linked RLC.

results obtained from the digests of whole myosin (Figure 5).

Photo-Cross-Linking of Myosin Containing Mutant RLC-C18. For RLC-C18, the photo-cross-linked products appeared as one band on SDS−PAGE. Although RLC-C18 was labeled with BPIA to the same extent (1 mol/mol), a substantial amount (~25%) remained un-cross-linked (Figure 7, lane b) under the same conditions used for RLC-C165 in the free state. In the bound state, the yield of the intrachain cross-linking further decreased when RLC-C18 was associated with the heavy chains, but the pattern remained the same as in the case of the free state (Figure 7, lane d). As in the case of RLC-C165, cross-linking between RLC-C18 and the heavy chains was not observed whether or not RLC-C18 was phosphorylated. However, myosin containing RLC-C18 formed additional cross-linked products which corresponded to the cross-linked regulatory light chains of two different heads of myosin; phosphorylation affected the mobility of the dimer band, suggesting a different cross-linking site may be involved in the phosphorylated state (results were not shown). Similar to the case of RLC-C165, phosphorylation had no effect on the intrachain cross-linking of RLC in the free state (Figure 7, lane c), whereas in the bound state, the intrachain cross-linking was almost completely inhibited in the phosphorylated state (Figure 7, lane e).

Identification of the Regions That Are Cross-Linked to Cys18. The bands corresponding to RLC and cross-linked

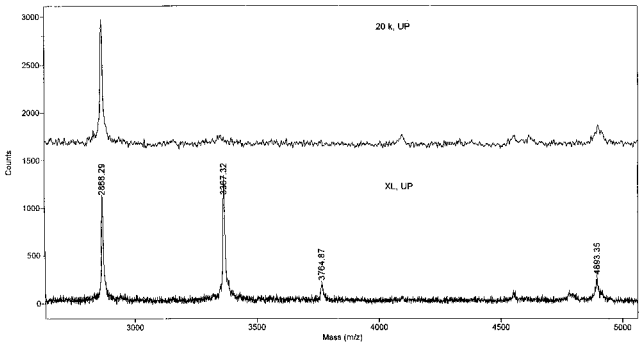

FIGURE 8: Mass analysis of the tryptic digests of cross-linked RLC-C18 (XL in Figure 7, lane d) on a MALDI-TOF mass spectrometer. Spectra were obtained from the HPLC fraction that eluted at 50−52 min of the tryptic digests of myosin containing unphosphorylated RLC-C18 before photolysis (top spectrum) and after photolysis (bottom spectrum). The complete spectra covered the mass range from 0 to 20 000 Da, and only the relevant sections are shown. The mass peak at 2868.29 Da was derived from internal standard bovine insulin with $2H^+$; the calculated value should be 2867.75 Da.

RLC (XL in Figure 7, lane d) of myosin were cleaved with trypsin, extracted, and then chromatographed separately on a Vydac column followed by analysis on a mass spectrometer. In this case of RLC-C18, the BP moiety is located in T8 (A17−K34), and therefore, any peptides that are cross-linked to Cys18 would have an additional mass of 2330.42 Da, the mass of T8 and the mass of benzophenone acetamide. In comparison with the spectrum of un-cross-linked RLC, the fraction that eluted at 50−52 min of cross-linked RLC showed two additional mass peaks at 3367.32 and 3764.87 Da (Figure 8). These two mass species matched well the calculated values of 3366.60 and 3764.93 Da, corresponding to T8 cross-linked to T15 and T16, respectively (Table 1). Similar results were obtained from the tryptic digests of photolyzed myosin (unphosphorylated). These two cross-linked fragments were too large to obtain useful information by PSD analysis. Therefore, in a separate experiment, the bands of cross-linked RLC-C18 (XL band in Figure 7, lane d) were cleaved with both trypsin and chymotrypsin followed by HPLC. The mass spectrum of the fraction that eluted at 46−47 min showed a peak with a mass of 1913.77 Da which

Table 3: Mass Ions of T15 and T15 Cross-Linked to ACSNVF(T8-C1)[b]

n	Fragments	b (cal)	observed	Fragments	y (cal)	observed	y* (cal)	observed
1	E	130.12	129.75	R	175.21	174.71	1051.02	
2	EL	243.28	243.05	DR	290.29	289.93	1166.10	
3	ELL	356.44	356.47	GDR	347.35	347.06	1223.16	
4	ELLT	457.55	457.16	MGDR	478.54		1354.35	1355.89
5	ELLTT	558.65	558.28	TMGDR	579.64		1455.45	
6	ELLTTM	689.84		TTMGDR	680.75		1556.56	1557.54
7	ELLTTMG	746.89		LTTMGDR	793.91		1669.72	1669.18
8	ELLTTMGD	861.98		LLTTMGDR	907.07		1782.88 1765.88[a]	1766.46
T15	ELLTTMGDR intact	1036.18		ELLTTMGDR minus-SCH_3	989.18	989.42	precursor	1913.77

[a] The calculated value of the y8* ion − 17 Da. [b] Values of y*n** ions were derived from the mass of the y*n* ion plus the mass of BP-T8-C1 (875.81 Da).

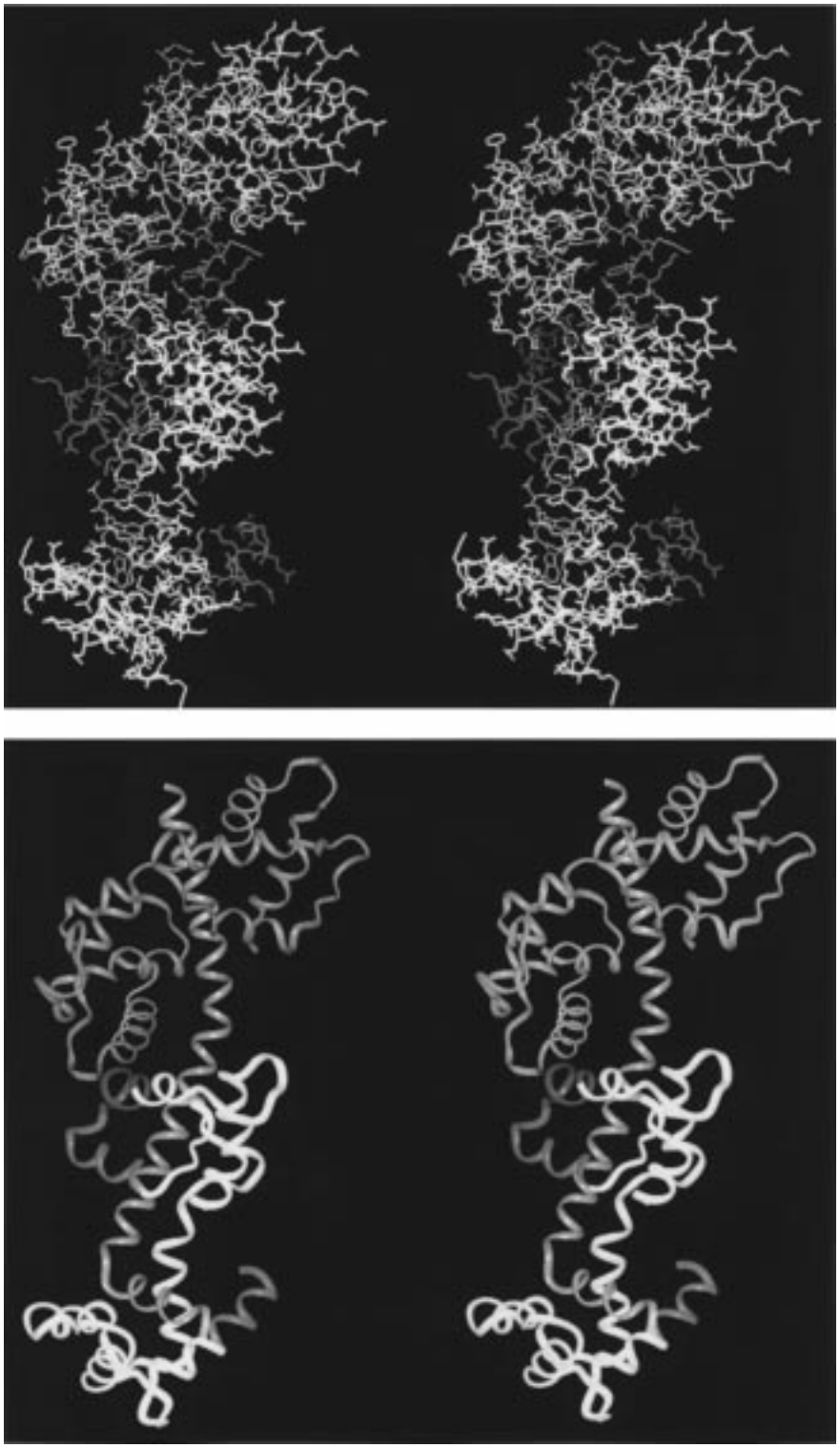

FIGURE 9: Stereoview of the atomic (A, top) and the ribbon (B, bottom) structures of the regulatory domain of scallop myosin (*8*). The essential light chain (brown) and regulatory light chain (yellow) wrap around the helical segment of the heavy chain (pink). The top of this figure is adjacent to the motor domain of myosin, and the bottom of this figure is next to the rod portion of myosin. The segment corresponding to Ala17−Lys34 of the RLC of the chicken gizzard myosin is colored in green. The segments corresponding to Glu124−Arg132 and Phe133−Arg143 are colored in light and dark blue, respectively. Amino acids corresponding to Cys18 and Cys165 are not in this structure. The side chains of the first and the last residues in this structure, Phe12 and Lys149 of the scallop RLC, corresponding to Phe25 and Lys163 of chicken gizzard RLC, respectively, are colored red (shown in panel A only). The image was created using Insight II from Biosym Technologies Inc. (San Diego, CA).

was very close to 1911.99 Da, the calculated mass of T15 cross-linked to Ala17−Phe21, the N-terminal portion of T8 and thus designated as T8-C1. PSD analysis of the precursor with a mass of 1913.77 Da showed b1−b5 ions and y1−y3 ions of T15 in addition to an ion with a mass of 989.42 Da which corresponded to the mass of T15 that lost the SCH_3 side chain (Table 3). Thus, the information obtained from PSD analysis not only confirmed that Cys18 was cross-linked to T15 in unphosphorylated myosin but also suggested that the first five residues from the N terminus and the last three

from the C terminus of the segment of Ala17−Phe21 were not involved in cross-linking and thus the sixth residue from the N terminus, Met129, was involved in cross-linking. Complementarily, ion masses matched y4*−y8* ions also appeared in the PSD analysis (Table 3), which demonstrated that all cross-linked products contained Met129 and further supported the notion that Cys18 was cross-linked to Met129.

From the tryptic and chymotryptic digests, the mass fragment corresponding to Ala17−Phe21 cross-linked to T16 was not detected; presumbly, this was due to an insufficient quantity.

DISCUSSION

Benzophenone iodoacetamide has been successfully used in detecting the nucleotide-induced conformational changes in myosin (*24*) and in function−structure relation studies of other proteins (*25*). However, the progress of this approach is hindered due to the fact that the identification of the cross-linking sites using the conventional method, microsequencing after isolation of the cross-linked peptides, is time-consuming, laborious, and sometimes not feasible if the yields of the cross-linked products are low. The technique of mass spectrometry made it possible to identify the peptides that were cross-linked to Cys165 and Cys18 without isolating each of them. The PSD analyses allowed us to further determine that Met129 and Met141 were cross-linked to Cys18 and Cys165, respectively. Although the side chain of methionine, SCH_3, is a preferable H donor for the photo-cross-linking reaction (*25*), the distance and the orientation between the benzophenone moeity and H donor are the dictating factor for the selectivity. Thus, the inhibition of cross-linking caused by phosphorylation reflects the spatial changes between Met129 and Met141 and Cys18 and Cys165. However, these changes most likely involve more than one residue; thus, the implication of our results on our understanding of the mechanism of phosphorylation regulation should not be limited to the residues that were involved in cross-linking.

Our results show that the stretch of residues Glu124−Arg143, in the F−G helix region of RLC, can be cross-linked to both N- and C-terminal segments of RLC with a benzophenone photo-cross-linker attached to Cys18 and Cys165, respectively, and this cross-linking is inhibited by the phosphorylation of Ser19. In contrast, photo-cross-linking between Cys165 and the N-terminal segment containing the phosphorylation site, Ala17−Lys34, is not affected by phosphorylation. These findings highlight certain spatial relationships within RLC in the inhibited and activated form of smooth muscle myosin. Most significantly, they suggest that upon phosphorylation the F−G helix region of RLC moves away from both termini of the molecule or, vice versa, a conformational change may underlie the activation of the smooth muscle myosin.

Early studies showed that calcium regulation in RLC-depleted scallop myosin can be restored by smooth muscle RLC (*26*) or by a chimeric RLC of skeletal myosin containing the third EF hand of the smooth muscle RLC (*27*). This suggests that RLC from chicken gizzard myosin has a structure similar to that of the scallop myosin and RLC of smooth muscle myosin could interact with the ELC and heavy chain in a manner similar to that in the scallop myosin. Our finding of inhibition of cross-linking between Cys18 and Cys165 and Glu124−Arg143 (Figures 1 and 9, colored in blue, corresponding to parts of the F helix, F−G linker, and G helix) in phosphorylated myosin shows that phosphorylated smooth myosin has a structure which is analogous to the Ca-bound state of the scallop myosin in which the residues in the F helix and the F−G linker of RLC are interacting with ELC and HC (*8*). One would expect that, in the absence of calcium, the interactions between RLC and ELC and HC are weaker in scallop myosin. Our results show that in unphosphorylated myosin Glu124−Arg143 can be cross-linked to Cys18 or Cys165, indicating that in the "off" state the F−G helix region is close to Cys18 and Cys165. In turn, this may lead to a weakening of the interactions between the F−G helix region and the ELC and HC, resulting in an inactive form of myosin. Although more experiments are needed to rule out other interpretations, the implication that maintaining the stable interactions between RLC and ELC and HC is critical for transmitting the phosphorylation effect is consistent with reports that the absence of the ELC resulted in myosin molecules that, although regulated by phosphorylation, had greatly reduced activities (*27*, *28*). The important role of the F−G helix region in phosphorylation regulation is consistent with the observation of Yang and Sweeney (*30*), who found that mutations in skeletal RLC impart phosphorylation-dependent regulation involving four sites in the F−G helix region.

The fact that cross-linking between Cys165 and the N-terminal stretch of Ala17−Lys34 is not affected by phosphorylation indicates that the N- and C-terminal segments of RLC remain in proximity regardless of the state of myosin. Previous studies on RLC mutants have shown that removal of 16 residues from the N terminus (*12*) or 23−26 residues from the C terminus (*12*, *31*) resulted in nonfunctional RLCs, indicating that both regions are required for myosin activity. In view of our present findings, it indicates that direct interactions between the N- and C-terminal regions are required for maintaining the proper conformation of myosin, both in the off and on states.

In conclusion, our results indicate that the N and C termini of RLC remain in proximity upon phosphorylation whereas phosphorylation induces change in the spatial relation between the Glu124−Arg143 and Cys18 and Cys165 regions, which reflects the switching between the off and on conformations of the smooth muscle myosin. In analogy to the crystal structure of the regulatory domain of the scallop myosin, our findings suggest that interactions between RLC and ELC and the heavy chain may play an important role in the activation of myosin.

ACKNOWLEDGMENT

We thank Lingjuan Ruan for generating the null cysteine mutant of the regulatory light chain in the initial stage of this work.

REFERENCES

1. Qian, F., Sukduang, S., Wong, A., and Lu, R. C. (1996) *Biophys. J. 70,* A3.
2. Wu, G., Wong, A., and Lu, R. C. (1997) *Biophys. J. 71,* A220.
3. Balint, M., Sreter, F., Wolf, I., Nagy, B., and Gergely, J. (1975) *J. Biol. Chem. 250,* 6168−6177.

4. Lu, R. C., Sosinski, J., Balint, M., and Sreter, F. (1978) *Fed. Proc. Am. Soc. Exp. Biol. 37*, 1695.
5. Adelstein, R. S., and Eisenberg, E. (1980) *Annu. Rev. Biochem. 49*, 921−956.
6. Pearson, R. B., Jakes, R., Kendrick-Jones, J., and Kemp, B. E. (1984) *FEBS Lett. 168*, 108−112.
7. Rayment, I., Rypniewski, W., Schmidt-Base, K., Smith, R., Tomchick, D., Benning, M., Winkelmann, D., Wesenberg, G., and Holden, H. (1993) *Science 261*, 50−58.
8. Xie, X., Harrison, D. H., Schlichting, I., Sweet, R. M., Kalabokis, V. N., Szent-Gyorgyi, A. G., and Cohen, C. (1994) *Nature 368*, 306−312.
9. Ho, S. N., Hunt, H. D., Horton, R. M., Pullen, J. K., and Pease, L. R. (1989) *Gene 77*, 51−59.
10. Studier, F. W., and Moffat, B. A. (1986) *J. Mol. Biol. 189*, 113−130.
11. Wolff-Long, V., Saraswat, L., and Lowey, S. (1993) *J. Biol. Chem. 268*, 23162−23167.
12. Ikebe, M., Ikebe, R., Kamisoyama, H., Reardon, S., Schwonek, J., Sanders, C., II, and Matsuura, M. (1994) *J. Biol. Chem. 269*, 28173−28180.
13. Perrie, W. T., and Perry, S. V. (1970) *Biochem. J. 119*, 31−38.
14. Graceffa, P. (1995) *J. Biol. Chem. 270*, 30187−30193.
15. Ikebe, M., Aiba, T., Onishi, H., and Watanabe, S. (1978) *J. Biochem. (Tokyo) 83*, 1643−1655.
16. Spudich, J. A., and Watt, S. (1971) *J. Biol. Chem. 246*, 4866−4871.
17. Graceffa, P. (1987) *FEBS Lett. 218*, 139−142.
18. Morita, J.-I., Takashi, R., and Ikebe, M. (1991) *Biochemistry 30*, 9539−9545.
19. Laemmli, U. K. (1970) *Nature 227*, 680−685.
20. Trybus, K. M., and Lowey, S. (1985) *J. Biol. Chem. 260*, 15988−15995.
21. Gharahdaghi, F., Kirchner, M., Fernandez, J., and Mishe, S. (1996) *Anal. Biochem. 233*, 94−99.
22. Cohen, S. L., and Chait, B. T. (1996) *Anal. Chem. 68*, 31−37.
23. Ikebe, M., and Hartshorne, D. J. (1985) *Biochemistry 24*, 2380−2387.
24. Lu, R. C., Moo, L., and Wong, A. (1986) *Proc. Natl. Acad. Sci. U.S.A. 83*, 6392−6396.
25. Dorman, G., and Prestwich, G. D. (1994) *Biochemistry 33*, 5661−5673.
26. Sellers, J. R., Chantler, P. D., and Szent-Gyorgyi, A. G. (1980) *J. Mol. Biol. 144*, 223−245.
27. Rowe, T., and Kendrick-Jones, J. (1992) *EMBO J. 11*, 4715−4722.
28. Trybus, K. (1994) *J. Biol. Chem. 269*, 20819−20822.
29. Katoh, T., and Morita, F. (1996) *J. Biol. Chem. 271*, 9992−9996.
30. Yang, Z., and Sweeney, H. L. (1995) *J. Biol. Chem. 270*, 24646−24649.
31. Trybus, K., and Chatman, T. (1993) *J. Biol. Chem. 268*, 4412−4419.
32. Messer, N. G., and Kendrick-Jones, J. (1988) *FEBS Lett. 234*, 49−52.
33. Reinach, F. C., and Fishman, D. A. (1985) *J. Mol. Biol. 181*, 411−422.
34. Goodwin, E. B., Szent-Gyorgyi, A. G., and Leinwand, L. A. (1987) *J. Biol. Chem. 262*, 11052−11056.

BI980054+